RSC Advances

ROYAL SOCIETY OF CHEMISTRY

www.rsc.org/advances

Ultrasonic assisted biodiesel production from waste cooking oil over synthesis of novel sulfonic functionalized carbon spheres derived from cyclodextrin via one-step: A way to produce biodiesel at short reaction time

Panya Maneechakr*, Jittima Samerjit* and Surachai Karnjanakom

Department of Chemistry, Faculty of Science, Rangsit University, Pathumthani 12000, Thailand

*Corresponding author.

E-mail addresses: panya.m@rsu.ac.th (P. Maneechakr); samerjit.j@gmail.com (J. Samerjit)

Abstract

In this study, a novel sulfonated carbon catalyst has been synthesized via one-step hydrothermal carbonization of cyclodextrin, hydroxyethylsulfonic acid and citric acid. The ultrasonic assisted biodiesel production from waste cooking oil in the existence of catalyst was investigated. The novel catalyst was characterized by BET, XRD, PSD, SEM-EDS, TGA, FT-IR, XPS and TPD. The catalyst exhibited a high acidity up to 1.87 mmol/g. 2^k factorial and Box-Behnken designs were applied to find the optimum conditions obtaining a maximum fatty acid methyl ester (FAME) yield. The result of the optimization implies that catalyst loading of 11.5 wt.%, reaction time of 8.8 min and reaction temperature of 117 °C provide a maximum FAME yield up to 90.8% in the ultrasonic assisted biodiesel production. The reusability of catalyst was studied for 4 cycles under optimum conditions and the results found that regenerated catalyst can be reused without any serious reduction of FAME yield. Kinetic studies showed that the reaction followed the first order reaction with activation energy of 11.64 kJ/mol.

Keywords: Ultrasonic assisted biodiesel production; cyclodextrin; 2^k factorial design; Box-Behnken design; Kinetic.

1. Introduction

The current declining reserves of fossil fuels have been concerned due to growing environment and technology. Recently, biofuels are considered to be one of further generation for alternative fuels because it can be generally found on the world, and also utilized easily.[1,2] Biodiesel is a kind of renewable energy for diesel engines, which is required for the transportation. Advantages of biodiesel are biodegradable, non-toxic, eco-friendly fuel.[3] There are potential feedstocks such as edible oils and non-edible oils.[4] The conventional edible oils have been identified such as palm oil, soybean oil and sunflower oil. However, waste cooking oil and non-edibles oil such as Jatropha oil and rubber seed oil have more attracted due to no effecting to food consumption.[5] For example, about 7 % of edible oil supplies were applied for biodiesel production in 2007, leading to state of food versus fuel issue. Therefore, this work has purposed to use the waste cooking oil as a raw material for biodiesel production which does not rely on the food supply as reported literatures.[6-8] Unfortunately, due to waste cooking oil has amount of high free fatty acids, it was limited with a wide range of base catalysts. As well known that saponification can be occurred between FFA and alkali catalyst to form the soap and the water.[9] To solve this problem, acid catalysts should be used. The conventional homogeneous acid catalysts are mostly used for biodiesel production such as HCl and H_2SO_4. However, the use of these catalysts causes many problems: (1) reactor corrosion, (2) large amount of waste water and (3) difficulty to reuse the catalysts, resulting in the increasing of overall cost for biodiesel production.[10,11] Recently, Lee and Yoo,[12] reported that heterogeneous catalysis was the most important technology in chemical industry as well as other environmental, energy applications, etc. Heterogeneous acid catalysts are offered as an optimum solution because they can eliminate such as corrosion, toxicity and separation. They also can be reused. Recently, heterogeneous acid catalysts were reported such as sulfonated zirconia, aminophosphonic acid resin D418,

amberlyst-15, SO_3H-SBA-15 and heteropolyacid catalyst.[13-17] Some catalysts limited due to low catalytic activity, low stability and high cost. Acid activated carbon derived from sugar and synthesized by sulfonation is regarded as a good catalytic performance for esterification. It has soft aggregate of polycyclic aromatic hydrocarbons rather than carbon material which directly obtained from lignocellulose.[18] Usually, its sulfonic group can be easily leached from structure when carried out at high temperature (>100 °C). For these reasons, glucose was used as carbon precursor for preparation of acid carbon catalyst. It was investigated and found that carbon material derived from glucose can form as a rigid structure composed of small poly cyclic aromatic carbon (a 3D sp^3-bonded structure) by hydrothermal carbonization. The hydrothermal carbonization method showed many advantages such as very cheap, mild, and absolutely "green" as it involves no catalyst, surfactant and organic solvent. Cyclodextrin (CD) is a new carbon precursor and catalyst to catalyze in the transesterification which has cyclic oligosaccharides structure of R-D-glucopyranose. It can produces into aromatic carbon spheres via hydrothermal carbonization.[19] The conventional surface modifications of the carbon materials involve the treatment with acids or ozone, thereby generating functionalities such as carboxylic acids, sulfuric acid and hydrochloric acid. In general, the sulfonated carbon-glucose was synthesized via two-step. First step, glucose was incompletely carbonized at high temperature for long time. Then sulfonation was taken to introduce the sulfonic acid groups in the second step. However, this method is required in harsh conditions for the inactive surface, gave the environmental unfriendly, the low product yield and the high numerous harmful wastes. Here, the novel catalyst has been synthesized via one-step hydrothermal carbonization of CD, hydroxyethylsulfonic acid and citric acid. The sulfonic group can be directly connected to the surface of the carbon during the carbonization process. Based on the structure of CD precursor, we are believed that it has higher catalytic activity and stability than conventional carbon catalyst for transesterification.

Ultrasonic irradiation technique on transesterification has shown the increase of reaction rate by order of magnitude due to a drastic increase in the interfacial area and improved heat/mass transfer phenomena and thermal/specific of mixing.[20,21] Ultrasound wave generates cavitation bubbles as it passes through the liquid. Ji *et al*.,[22] investigated the influences of sonication, mechanical stirring and hydrodynamic cavitation on the biodiesel production from soybean oil by KOH catalyst. They were found that ultrasonic method provided shorter reaction time and higher biodiesel yield when compared with the conventional mechanical stirring. Stavarache *et al*.,[23] also reported that ultrasonic method gave better results such as lower reaction time, lower reaction temperature, lower catalyst loading and higher FAME yield, resulting from the immiscible liquids and intensified reaction. Moreover, Choedkiatsakul *et al*.,[24] studied the further improvement with transesterification of palm oil by incorporation of mechanical stirring into the ultrasonic reactor. Recently, many researchers have studied biodiesel production from edible-oils and non-edible oils by using heterogeneous catalysts with sonication method.[25] Shahraki *et al*.,[26] reported that sono-synthesis of biodiesel from soybean oil achieved with catalysis by KF/γ-Al_2O_3. Pukale *et al*.,[27] studied transesterification of waste cooking oil in the presence of heterogeneous solid catalyst. The optimum conditions such as catalyst concentration of 3 wt.% K_3PO_4 and reaction time of 90 min gave a highest FAME yield up to 92.0%. Kumar *et al*.,[28] reported that ultrasonic-assisted transesterification of *Jatropha curcus* oil using Na/SiO_2 catalyst was environmental, ecologically and economically friendly process. To date, very few studies focused on the ultrasonic assisted biodiesel production from waste cooking oil, especially with using heterogeneous catalyst.[29] No study has been reported on the biodiesel production over sulfonated solid carbon derived from cyclodextrin (SO_3H-CD) with ultrasonic system. The main objective of this work was to optimize of ultrasonic assisted biodiesel production via a single-step process using SO_3H-CD catalyst. Experimental design

was investigated.[30] A 2^k factorial design was used to screen the significant factor. Response surface methodology (RSM) was applied to find the levels of optimum conditions using a Box-Behnken design. The SO_3H-CD catalyst was characterized by BET, XRD, PSD, SEM-EDX, TGA, FT-IR, XPS, NH_3-TPD and titration. The catalyst reusability was studied. Moreover, a kinetic model was investigated and the kinetic parameters were determined by fitting the model with the experimental results.

2. Experimental

2.1. Materials

Waste cooking oil was obtained from local restaurants in Thailand. The properties of waste cooking oil are shown in Table S1. Hydroxyethylsulfonic acid was obtained from synthesis of mercaptoethanol and 5 vol.% H_2O_2 via oxidation reaction. Cyclodextrin (≥98% reagent grade), methanol (99.8% reagent grade), citric acid (≥99.5% reagent grade), sulfuric acid (95-98% AR grade) and methyl heptadecanoate (≥99% reagent grade) were purchased from Sigma-Aldrich.

2.2. Catalyst preparation

Firstly, 10 g of CD, 3 g of hydroxyethylsulfonic acid, 5 g of citric acid and 80 mL of DI water were mixed and stirred at ambient temperature for 1 h. The mixture solution was added in a Teflon-lined stainless steel autoclave and heated at 180 °C for 4 h. Then the black slurry was filtered, washed with 1000 mL of DI water and dried at 105 °C to obtain sulfonated solid carbon. The sulfonated solid carbon derived from CD was initialized as SO_3H-CD catalyst.

2.3. Characterization of catalyst

The Brunauer–Emmett–Teller (BET) surface area and the Barrett–Joyner–Hallenda (BJH) pore size of catalyst were measured by N_2 adsorption and desorption at liquid nitrogen temperature of -196 °C. The crystalline structure of catalyst was analyzed by powder X-ray diffraction (XRD). The particle-size distribution (PSD) of catalyst was measured by a particle size analyzer (Malvern/Mastersizer X). The morphology of catalyst was characterized by a scanning electron microscope (SEM) equipped with energy dispersive spectroscopy (EDS). The thermal stability of catalyst was determined by thermo-gravimetric analysis (TGA). The FT-IR spectra of sulfate group in the catalyst were analyzed using a Perkin Elmer Spectrum 100 FTIR spectrometer. The graphitization degree was accessed by X-ray photoelectron spectroscopy (XPS). The acid density of catalyst was analyzed by NH_3-temperature programmed desorption (NH_3-TPD) and titration.

2.4. Experimental procedure

The transesterification reaction was performed in a 250 mL three-neck round bottom flask equipped with an ultrasonic probe , a condenser and thermocouple thermometer (Fig. S1). In each experiment, a frequency of ultrasonic probe and a stirring speed were fixed at 25 kHz and 800 rpm, respectively. The effects of catalyst loading (5-15 wt.%), reaction time (2-14 min), reaction temperature (50-150 °C) and molar ratio of methanol to oil (20:1-40:1) on the FAME yield were investigated using statistical analysis design. After finishing the transesterification reaction, the spent catalyst was separated from the mixture by centrifugation. The filtrate was separated into two layers using a separation funnel. The upper layer or FAME was performed under rotary evaporation to remove the remaining methanol and water. Finally, the obtained FAME was filtered with sodium sulfate before gas chromatography (GC) analysis. The FAME product was determined by GC (Agilent 7820A), equipped with a flame ionization detector and a capillary column (DB-WAX, 30 m × 0.25

mm × 0.25 μm), following the standard method of EN 14103 with the use of methyl heptadecanoate (C17:0) as an internal standard.

The percentage of FAME yield was calculated by following Eq. (1):

$$\text{FAME yield (\%)} = \frac{(\sum A) - A_{\text{EI}}}{A_{\text{EI}}} \times \frac{C_{\text{EI}} \times V_{\text{EI}}}{W_{\text{s}}} \times \frac{W_{\text{P}}}{W_{\text{O}}} \times 100 \quad (1)$$

where ΣA is the total peak area of FAME product, A_{EI} is the peak area of C17:0, C_{EI} is the concentration of C17:0 (mg/mL), V_{EI} is the amount of C17:0 (mL), W_{S} is the weight of sample (mg), W_{P} is the weight of produced FAME (mg) and W_{O} is the weight of used oil.

2.5. Catalyst reusability

After finishing the reaction, the spent catalyst was washed with acetone to remove glycerin and any undesired materials attached on the surface. The spent catalyst was regenerated by soaking with conc. H_2SO_4. To study the long-term stability of catalyst, it was reused up to 4 cycles. The regenerated catalyst was investigated to compare with the catalyst without regeneration on the response of FAME yield.

2.6. Experimental design

The purpose of the design was to investigate the significance of process factor and to optimize the biodiesel production over SO_3H-CD catalyst by employing a single-step process under ultrasonic condition.

A 2^4 factorial design was used to screen the significant factors and to increase the model accuracy. Four factors such as catalyst loading (X_1), reaction time (X_2), reaction temperature (X_3) and molar ratio of methanol to oil (X_4) were designed by consisting of 16 experiments with their low and high values. The ranges of full factorial design of each factor

are shown in Table 1. The regression model for screening the factors was expressed as following Eq. (2):

$$Y = \beta_0 + \sum_{i=1}^{k} \beta_i X_i + \sum_{i<j}\sum \beta_{ij} X_i X_j \quad (2)$$

Where Y is the FAME yield (%), β_0 is the constant coefficient, β_i is the coefficient for the linear effect, β_{ij} is the coefficient for the interaction effect and X_i and X_j are the factor codes.

Investigating a Box-Behnken design required 15 experiments with three factors in this research (Table 2). This design was studied the response pattern and to find the optimum condition together with maximum FAME yield. Table 2 shows the ranges and levels of factors. The Box-Behnken model for optimizing the factors was expressed as following Eq. (3):

$$Y = \beta_0 + \beta_1 X_1 + \beta_2 X_2 + \beta_3 X_3 + \beta_{11} X_1^2 + \beta_{22} X_2^2 + \beta_{33} X_3^2 + \beta_{12} X_1 X_2 + \beta_{13} X_1 X_3 + \beta_{23} X_2 X_3 \quad (3)$$

Where Y is the FAME yield (%), β_0 is the constant coefficient, β_1, β_2 and β_3 are coefficients for the linear effects, β_{11}, β_{22} and β_{33} are the coefficients for the quadratic effects, β_{12}, β_{13} and β_{23} are the coefficients for the interaction effects and X_1,X_2 and X_3 are the factor codes.

2.7. Kinetic modeling

The kinetic study for the transesterification reaction was carried out to continuously investigate after optimization process achieved. The stoichiometry of three step and overall transesterification reaction can be written as following Eqs. (4) and (5):

$$\text{Triglyceride} + CH_3OH \underset{k_4}{\overset{k_1}{\leftrightarrow}} R_1COOH_3 + \text{Diglyceride}$$
$$\text{Diglyceride} + CH_3OH \underset{k_5}{\overset{k_2}{\leftrightarrow}} R_2COOH_3 + \text{Monoglyceride} \quad (4)$$
$$\text{Monoglyceride} + CH_3OH \underset{k_6}{\overset{k_3}{\leftrightarrow}} R_3COOH_3 + \text{Glycerol}$$
$$\text{Triglyceride} + 3CH_3OH \underset{k_8}{\overset{k_7}{\leftrightarrow}} 3RCOOH_3 + \text{Glycerol} \quad (5)$$

From above stoichiometry, the conversion of waste cooking oil into FAME was determined as the total mol of $RCOOH_3$ or FAME divided by total mol of triglycerides (Eq. (6)).

Conversion (%) = [Total mol of FAME produced/3 × (Total mol of triglyceride)] × 100 (6)

The reaction rate was determined as following Eq. (7):

$$-\frac{dC_A}{dt} = k_7 C_A^X C_B^Y - k_8 C_C^W C_D^Z \quad (7)$$

where C_A, C_B, C_C and C_D are the concentrations of triglyceride, methanol, glycerol and FAME, respectively. W, X, Y and Z refer to their reaction order. k_7 and k_8 are the kinetic constants for the forward and backward reaction, respectively.

From the Eq. (7), it can be reduced to:

$$-\frac{dC_A}{dt} = k' C_A^n \quad (8)$$

where $k' = k_7 C_B^Y$ and/or k' is modified rate constant. Due to the used molar ratio of methanol to oil was much higher than other components, therefore, $k_7 C_B^Y$ can be constant. Moreover, k_7 is also much higher than k_8.[31]

$$C_A = C_{A0}(1 - X) \quad (9)$$

where C_{A0} and X are the initial concentration of triglyceride and the conversion of oil or triglyceride into FAME, respectively. Therefore, the overall reaction rate can be summarized and expressed as following Eq. (10):

$$\frac{dX}{dt} = \frac{k'}{C_{A0}}[C_{A0}(1-X)]^n = k''[C_{A0}(1-X)]^n \quad (10)$$

When $k'' = k'/C_{A0}$ and $n = 1$, thus, Eq. (10) can be rearranged and integrated to obtain as following Eq. (11):

$$\ln(1-X) = k't \quad (11)$$

In case that $n \neq 1$, rearranging and integrating of Eq. (10) can be obtained as following Eq. (12):

$$(1-X)^{(1-n)} = 1 + (n-1)k''C_{A0}^{n}t \quad (12)$$

From above equation, the best straight line was determined from line based on highest R^2 close to 1. According to Arrhenius equation, the reaction rate can be expressed as a function of temperature in the following Eq. (13):

$$\ln k' = -\frac{E_a}{RT} + \ln A \quad (13)$$

where E_a is the activation energy (kJ/mol), A is the pre-exponential factor (min^{-1}), R is the gas constant (8.314 J/Kmol) and T is the reaction temperature (K).

3. Results and discussion

3.1. Characterization of catalyst

Fig. 1A shows the XRD patterns of catalyst. The broad diffraction peak at 10-30° was assigned to (002) plane of the carbon in CD. After sulfonation, the mentioned (002) diffraction peak was shifted to the larger 2θ angle, suggesting that the carbonization may be occurred during the sulfonation process with concentrated acid resulted in smaller polycyclic carbon ring.[19] Fig. 1B shows the particle-size distribution of catalyst. It was found to be in the range of 0-15 μm. This result was related with SEM image in Fig. 1C. Moreover, it was found to be regular particle shape of sphere carbon with the existence of S element, suggesting that rich sulfonic group attached on the surface of catalyst. Figure 1D shows TGA patterns of CD-carbon and SO_3H-CD catalyst. The initial weight loss in the temperature ranges of 0-120 °C due to loss of water. Gradual weight loss of SO_3H-CD at higher temperature ≥ 280 °C shows the decomposition of sulfonic group. It should be noted that SO_3H-CD catalyst had the thermal stability at temperatures closes to 280 °C under oxygen-free conditions. The FTIR spactra of catalyst is shown in Figure 1E. The strong bands at 1040 cm^{-1} and 940 cm^{-1} could be identified to the stretching modes of sulfate groups. This evidence indicates that the sulfuric resulted in extensive covalent sulfonation of carbonized CD catalyst. Parthiban and Perumalsamy,[4] reported that sulfonic acid group coupled with carbon ring can be formed a stable covalent structure, leading to good stability maintaining at high reaction temperature. The XPS spactra are presented in Fig. 1F. The S_2p photoelectron peak at 168 eV and the inserted O_{1s} photoelectron peak at 531.6 eV were attributed to the carbon material containing sulfonic group. Fig. 1G shows NH_3-TPD profile of catalyst. The NH_3-TPD profile showed that three acid sites, a weak acid (70-150 °C), a medium acid (170-240 °C) and strong acid (270-320 °C) were observed. The BET surface area and pore size of SO_3H-CD catalyst were determined to be 8.2 m^2/g and 22.1 nm, respectively (Table 3). The titration result found that high $–SO_3H$ density of fresh catalyst was 1.87 mmol/g. It should be noted that the low surface area and large pore size can increase the accessibility of sulfuric acid into the carbon bulk,

which would give a higher concentration of covalently bonded carbon with a sulfonic group. Moreover, due to large pore size obtained, reactant such as oil and methanol can be easily diffused into the internal of catalyst structure, resulting in the increase of catalytic activity.[32-34] Shuit *et al*.,[35] reported that low surface and narrow pore size of solid catalysts exhibited a mass transfer resistance because of the presence of a three phase system as oil, methanol and solid catalyst in the reaction mixture that limits the pore diffusion process and reduces the active sites available for the catalytic reaction, thereby decreasing the reaction rate.

3.2. Ultrasonic assisted biodiesel production with statistical analysis

Using a 2^4 factorial design, 16 experiments were carried out and provided the responses as experimental FAME yields (Table 1). To screen the significant factors, estimate values were plotted versus normal probability (Fig. 2). As shown in Fig. 2, it was clearly seen that catalyst loading, reaction time, reaction temperature and their interactions had a significant effect on ultrasonic assisted biodiesel production, while the ranges of molar ratio of methanol to oil had no effect on the FAME yield. One can see that this work used the ranges of molar ratio of methanol to oil (20:1-40:1) which is an excess amount, leading to shift forward equilibrium to the FAME product. It should be note that remaining amount of methanol can be recovered from the mixture by evaporation. The X_3 factor or reaction temperature had a most effect on biodiesel production, suggesting that transesterification reaction required high temperature due to its endothermic nature. Table S2 shows the analysis of variance (ANOVA) for 2^4 factorial design. The confidence level for all stages was determined at 95%. The F-value more than 5.32 indicated model terms are significant. The summary of ANOVA provided a result according with normal probability graph in Fig .2. The regression model was determined using a significant coefficient, which model can be expressed in team of liner equation as following Eq. (14):

$$Y = 63.98 + 5.77X_1 + 7.955X_2 + 17.63X_3 - 6.42X_1X_2 - 2.655X_1X_3 - 3.42X_2X_3 + 0.845X_1X_2X_3 \quad (14)$$

where Y is the FAME yield (%), X_1 is the catalyst loading (wt.%), X_2 is the reaction time (min) and X_3 is the reaction temperature (°C). The regression model was also applied for calculation of predicted values. Fig. 3A shows the normal probability of residuals. It was found to be well fitted with R^2 close to 1 (R^2 = 0.9590). Moreover, Fig. 3B also represents residual distribution of model did not follow a particular trend with respect to predicted values, indicating that this model has dependability and acceptable. Here, a lowest molar ratio of methanol to oil (20:1) was selected and fixed for optimization and kinetic process.

The experimental design for optimization of ultrasonic assisted biodiesel production from waste cooking oil over SO_3H-CD was a Box-Behnken design. In this work, Box-Behnken design is a combination between 2^k factorial design with an incomplete block design, providing to 15 experiments. Based on this design and experimental results are shown in Table 2. The quadratic regression model for determination of predicted values is given as following Eq. (15):

$$Y = 87.7 + 7.675X_1 + 3.938X_2 + 6.513X_3 - 9.25X_1^2 - 6.225X_2^2 - 6.525X_3^2 - 2.575X_1X_2 - 5.175X_1X_3 - 3.1X_2X_3 \quad (15)$$

where Y is the FAME yield (%), X_1 is the catalyst loading (wt.%), X_2 is the reaction time (min) and X_3 is the reaction temperature (°C).

Fig. 4 shows the plot between experimental and predicted FAME yields. As expected, the predicted values are well close to the experimental values, providing a value of R^2 = 0.9770, indicating that the fitted model could explain 97.70% of the variability. The effects of catalyst loading and reaction time on ultrasonic assisted biodiesel production at a constant

reaction temperature of 100 °C are presented in Fig. 5A. As expected, increasing the catalyst amount enhances the FAME yield because an increase in the active sites for the reaction. Moreover, it may be due to the fact that addition of excess catalyst loading results in faster reaction of esterification and transesterification which increases the FAME yield. However, the trend was reversed when the catalyst loading reached a certain amount, resulting from over catalyst loading would make the esterification of free fatty acid progress faster and more water could be easily formed in a shorter time. As well known that the excess water amount could lead to deactivation of the catalyst due to hydration reaction occurred. The sulfonic acid-catalyzed esterification mechanism consists of protonation of the free fatty acid with the catalyst. The accessibility of alcohol on the carbocation leads to the occurrence of tetrahedral intermediate and releasing of water (Fig. 6). The mechanism was also related on theoretical alcohol adsorption mechanisms of Langmuir–Hinshelwood and Eley–Rideal.[36,37] In addition, it is possible that the increase of catalyst amount affected the some problems such as phase separation and more glycerol amount, presenting under unsuitable conditions. The reaction time presented a positive influence on the FAME yield but had less effect than catalyst loading as it can be observed in Fig. 5A. At too long reaction time, it could promote the backward reaction with decreasing of FAME yield. This promoting was explained by influence of ultrasonic energy increasing in interfacial area and activity of the microscopic and macroscopic bubbles formed when ultrasonic waves were applied in the three-phase reaction system.[38] The bubbles will be formed and undergoes breakdown after an approximate period at 400 ms, resulting in small hotspots that can offer the energy for some chemical reactions (Fig. S2). The effects of catalyst loading and reaction temperature on ultrasonic assisted biodiesel production at a constant reaction time of 8 min are presented in Fig. 5B. The FAME yield was increased significantly when catalyst loading and reaction temperature increased with their optimum conditions were 12 wt.% and 120 °C, respectively,

providing a maximum FAME yield (90%) as it can be observed in Fig. 5B. Fig. 5C shows the effects of reaction time and reaction temperature at a constant catalyst loading of 10 wt.%. As shown in Fig. 5C, a maximum FAME yield was obtained to be 89.6 % with a reaction time and a reaction temperature were 9.2 min and 120 °C, respectively. One can see in Fig. 5B and C that the reaction temperature fixed a constant at 120 °C. It should be noted that as beyond temperature, it could occur the frying process and/or some chemical reactions such as thermolytic, hydrotic and oxidative reactions. Moreover, it can be attributed the evaporation of methanol as vapor phase in reactor system, leading to less available in reaction environment.[31] Based on the quadratic regression model, the predicted maximum FAME yield of 90.3% was achieved under the optimum conditions: catalyst loading of 11.5 wt.%, reaction time of 8.8 min and reaction temperature of 117 °C. To confirm the prediction of model, the optimum conditions were tested up to three replicates for biodiesel production. The average FAME yield form actual experiment was obtained to be 90.8% indicating that experimental value closed to predicted value. For comparison, optimum condition of experiment was compared with without ultrasonic system using heating and stirring methods. The FAME yield was reduced to about 56% with without ultrasonic system, suggesting that longer reaction time was necessary. As a result, the use of ultrasonic system is beneficial in both of the FAME yield as well as the rate of reaction.

3.3. Catalyst reusability

The influences of catalyst reusability on ultrasonic assisted biodiesel production are illustrated in Fig. 7. One can see that a significant reduction in catalytic activity was detected catalyst without regeneration. The reduction of FAME yield in each cycle could be explained attending to different possibilities: (1) the deactivation of active sites due to their poisoning by some molecules present in the reaction mixture such as ion-exchange between alkali cations with protons and natural adsorption of reactants and products in system and (2) the

dependency of acid loss with temperature and sonic suggests acid sites are reacting, for instance with alcohol to lead methyl sulfonates (Fig. S3). However, in this case, a regeneration process as via repeating sulfonation could be applied to solve the deactivation problems of catalyst. As shown in Fig. 7, for catalyst after regeneration, no serious reduction on FAME yield was observed in very cycles, suggesting that catalyst after regeneration could exist in the presence of sulfonic group, which this ascription was confirmed by titration and elemental analysis results in Table 3. Moreover, the presence of Na element on the surface of spent catalyst (4th reuse) without regeneration can be clearly found on SEM-EDS result in Fig. S4. However, with spent catalyst (4th reuse) after regeneration, one can see that a little amount and/or almost disappearance of Na element together with an increasing of S amount were observed, resulting from the sulfonation with ion-exchange nature. For comparison of catalytic activity, the commercial catalysts such as Amberlyst-15 (4.5 mmol/g of acidity and 45 m^2/g of surface area), zeolite (HY) (0.33 mmol/g of acidity and 425 m^2/g of surface area), γ-Al_2O_3 (0.31 mmol/g of acidity and 221 m^2/g of surface area) and CD-carbon derived from hydrothermal carbonization of CD and water (0.02 mmol/g of acidity and 11 m^2/g of surface area) were tested for the transesterification of waste cooking oil. As shown in Fig. S5, SO_3H-CD exhibited better catalytic activity than other catalysts. The CD-carbon obtained from single cyclodextrin showed almost no catalytic activity, resulting from its low acidity. This is probably due to their acidity promote the activity for transesterification. To confirm the influence of acidity, SO_3H-CD was synthesized with different acid densities, following with acid densities on catalyst reusability result. As shown in Fig.S6, it can be seen that the increase of FAME yield was related with increasing of acid densities. This result was corresponded with catalyst reusability result. Moreover, it also believed that the outer layer of SO_3H-CD carbon sphere consists of active site and hydrophilic group such as sulfonic group, carboxylic group and hydroxyl group while inner layer consists of hydrophobic group such as

polyaromatics could promote the effect of mass transfer, leading to the higher catalytic performance.

3.4. Kinetic of the transesterification process

In the present study, kinetic of transesterification reaction was investigated as a function of temperatures with times in the range between 60 to 120 °C and 2 to 10 min, respectively. The optimum catalyst loading (11.5 wt.%) was fixed. As shown in Fig. 8, it indicated that the transesterification catalyzed by CD-SO_3H and assisted by ultrasonic system occurred in a first order reaction due to kinetic data curves in each temperature fitted with R^2 > 0.99. According to previous report of Freedman et al.,[39] they found that acid catalyzed transesterification process was a first order reaction. After fitting data in Fig. 8, different temperatures with reaction rate constants are given in Table 4. Based on the data in Table 4, due to the considerable effect of reaction temperature on rate constant, the relationship between them was obeyed using the Arrhenius law (Eq. 13). Fig. 9 shows the graph plotted between the natural logarithm of reaction rate constant (ln k') versus the inverse of temperature (1/T). The activation energy (E_a = 11.64 kJ/mol) and pre-exponential factor (A = 3.14 min^{-1}) was obtained from slope and intercept of Arrhenius plot, respectively. The activation energy values in the range of 33-84 kJ/mol have been reported for acid-base catalyzed homogeneous transesterification of edible oil.[39,40] Uzun et al.,[41] reported that the activation energy of alkali-catalyzed transesterification of waste frying oils (WFO) was 11.7 kJ/mol. The activation energy was reported value of 70.6 kJ/mol for alkaline ethanolysis of castor oil.[42] For heterogeneous catalyst, Kumar and Ali,[43] reported that the activation energy of transesterification using nanocrystalline K-CaO catalyst was found to be 54 kJ/mol. The activation energy for the Zr/CaO catalyzed methanolysis and ethanolysis was found to be 29.8 kJ/mol and 42.5 kJ/mol, respectively.[44] Kansedo and Lee,[45] reported that activation energy of 36.03 kJ/mol and pre-exponential factor of 5.56 × 102 min^{-1} were obtained using

sulfated zirconia catalyst for biodiesel production from non-edible sea mango oil. It should be noted that the range of activation energy (26-84 kJ/mol) reported for heterogeneous catalysts with transesterification reaction. These evidences indicated that the activation energy of this work was observed outside the range of reported values. This is due to the effect of the reduction of the mass transfer resistances which helped by cavitation process of intense turbulence and micro-scale liquid circulation. Based on the fitting Eq. (16), it was clearly confirmed that ln *k* changed linearly with 1/T in the studied temperature range as expected for a single rate-limited thermally activated process.

$$\ln k' = -\frac{1.4}{T} + 1.444 \ \ (R^2 = 0.9953) \tag{16}$$

Moreover, reaction temperature was proved to be a positive effect which was closely relative with the conversion efficiency of transesterification process. The FAME or biodiesel product was tested by comparing with American ASTM D 6751 standard (Table 5). The properties of biodiesel produced in this work met the criteria of ASTM standard. From this result, it could be rated as a realistic alternative to petroleum diesel.

4. Conclusions

In the present study, ultrasonic assisted transesterification process catalyzed by SO_3H-CD was proved to be a high performance technology for biodiesel production. The catalyst was characterized by BET, XRD, PSD, SEM-EDS, TGA, FT-IR, XPS and TPD. The statistical analyses were clarified by $R^2 > 0.95$. The maximum FAME yield was 90.8% at optimum conditions: catalyst loading of 11.5 wt.%, reaction time of 8.8 min and reaction temperature of 117 °C. The high stability and catalytic performance of catalyst showed excellent after the regeneration. The SO_3H-CD showed better catalytic performance when compared with commercial catalysts. Kinetic studies showed that the reaction followed the

first order reaction with activation energy of 11.64 kJ/mol and pre-exponential factor of 3.14 min^{-1}.

Acknowledgments

The authors wish to acknowledge Department of Chemistry, Faculty of Science, Rangsit University for supporting all instruments and chemicals.

References

1 D. Simionato, S. Basso, G. M. Giacometti and T. Morosinotto, *Biophys. Chem.*, 2013, **182**, 71–78.

2 I. M. R. Fattah, M. A. Kalam, H. H. Masjuki and M. A. Wakil, *RSC Adv.*, 2014, **4**, 17787–17796.

3 S. B. Lee, K. H. Han, J. D. Lee and I. K. Hong, *J. Ind. Eng. Chem.*, 2010, **16**, 1006–1010.

4 K. S. Parthiban and M. Perumalsamy, *RSC Adv.*, 2015, **5**, 11180–11187.

5 V. G. Gude and G. E. Grant, *Appl. Energy*, 2013, **109**, 135–144.

6 N. Kaur and A. Ali, *Appl. Catal., A*, 2015, **489**, 193–202.

7 N. Kaur and A. Ali, *RSC Adv.*, 2015, **5**, 13285–13295.

8 M. Kaur and A. Ali, *Eur. J. Lipid Sci. Technol.*, 2015, **117**, 550–560.

9 W. Y. Lou, M. H. Zong and Z. Q. Duan, *Bioresour. Technol.*, 2008, **99**, 8752–8758.

10 J. Chen, L. Jia, X. Guo, L. Xiang and S. Lou, *RSC Adv.*, 2014, **4**, 60025–60033.

11 I. M. Atadashi, M. K. Aroua, A. R. A. Aziz and N. M. N. Sulaiman, *J. Ind. Eng. Chem.*, 2013, **19**, 14–26.

12 D. W. Lee and B. R. Yoo, *J. Ind. Eng. Chem.*, 2014, **20**, 3947–3959.

13 Y. Zhang, W. T. Wong and K. F. Yung, *Appl. Energy*, 2014, **116**, 191–198.

14 P. Yin, L. Chen, Z. Wang, R. Qu, X. Liu, Q. Xu and S. Ren, *Fuel*, 2012, **102**, 499–505.

15 M. Li, Y. Zheng, Y. Chen and X. Zhu, *Bioresour. Technol.*, 2014, **154**, 345–348.

16 D. Zuo, J. Lane, D. Culy, M. Schultz, A. Pullar and M. Waxman, *Appl. Catal., B*, 2013, **129**, 342–350.

17 A. S. Badday, A. Z. Abdullah and K. T. Lee, *Appl. Energy*, 2013, **105**, 380–388.

18 M. Hara, *Top. Catal.*, 2010, **53**, 805–810.

19 X. B. Fu, J. Chen, X. L. Song, Y. M. Zhang, Y. Zhu, J. Yang and C. W. Zhang, *J. Am. Oil Chem. Soc.*, 2015, **92**, 495–502.

20 G. Chen, R. Shan, J. Shi and B. Yan, *Bioresour. Technol.*, 2014, **171**, 428–432.

21 M. Maghami, S. M. Sadrameli and B. Ghobadian, *Appl. Therm. Eng.*, 2015, **75**, 575–579.

22 J. Ji, J. Wang, Y. Li, Y. Yu and Z. Xu, *Ultrason. Sonochem.*, 2006, **44**, e411–e414.

23 C. Stavarache, M. Vinatoru, R. Nishimura and Y. Maeda, *Ultrason. Sonochem.*, 2005, **12**, 367–372.

24 I. Choedkiatsakul, K. Ngaosuwan, G. Cravotto and S. Assabumrungrat, *Ultrason. Sonochem.*, 2014, **21**, 1585–1591.

25 M. Takase, Y. Chen, H. Liu, T. Zhao, L. Yang and X. Wu, *Ultrason. Sonochem.*, 2014, **21**, 1752–1762.

26 H. Shahraki, M. H. Entezari and E. K. Goharshadi, *Ultrason. Sonochem.*, 2015, **23**, 266–274.

27 D. D. Pukale, G. L. Maddikeri, P. R. Gogate, A. B. Pandit and A. P. Pratap, *Ultrason. Sonochem.*, 2015, **22**, 278–286.

28 D. Kumar, G. Kumar, Poonam and C. P. Singh, *Ultrason. Sonochem.*, 2010, **17**, 839–844.

29 S. M. Hingu, P. R. Gogate and V. K. Rathod, *Ultrason. Sonochem.*, 2010, **17**, 827–832.

30 P. Kumar, M. Aslam, N. Singh, S. Mittal, A. Bansal, M. K. Jha and A. K. Sarma, *RSC Adv.*, 2015, **5**, 9946–9954.

31 A. Talebian-Kiakalaieh, N. A. S. Amin, A. Zarei and I. Noshadi, *Appl. Energy*, 2013, **102**, 283–292.

32 Q. Shu, Q. Zhang, G. Xu, Z. Nawaz, D. Wang and J. Wang, *Fuel Process. Technol.*, 2009, **90**, 1002–1008.

33 Q. Shu, Z. Nawaz, J. Gao, Y. Liao, Q. Zhang, D. Wang and J. Wang, *Bioresour. Technol.*, 2010, **101**, 5374–5384.

34 Q. Shu, J. Gao, Z. Nawaz, Y. Liao, D. Wang and J. Wang, *Appl. Energy*, 2010, **87**, 2589–2596.

35 S. H. Shuit, K. F. Yee, K. T. Lee, B. Subhash and S. H. Tan, *RSC Adv.*, 2013, **3**, 9070–9094.

36 S. Miao and B. H. Shanks, *J. Catal.*, 2011, **279**, 136–143.

37 Y. Liu, E. Lotero and J. G. Goodwin Jr, *J. Catal.*, 2006, **242**, 278–286.

38 H. Mootabadi, B. Salamatinia, S. Bhatia and A. Z. Abdullah, *Fuel*, 2010, **89**, 1818–1825.

39 B. Freedman, R. O. Butterfield and E. H. Pryde, *J. Am. Oil Chem. Soc.*, 1986, **63**, 1375–1380.

40 H. Noureddini and D. Zhu, *J. Am. Oil Chem. Soc.*, 1997, **74**, 1457–1463.

41 B. B. Uzun, M. Kılıç, N. Özbay, A. E. Pütün and E. Pütün, *Energy*, 2012, **44**, 347–351.

42 N. D. L. D. Silva, C. B. Batistella, R. M. Filho and M. R. W. Maciel, *Energy Fuels*, 2009, **23**, 5636–5642.

43 D. Kumar and A. Ali, *Biomass Bioenergy*, 2012, **46**, 459–468.

44 N. Kaur and A. Ali, *Fuel Process. Technol.*, 2014, **119**, 173–184.

45 J. Kansedo and K. T. Lee, *Chem. Eng. J.*, 2013, **214**, 157–164.

Table captions

Table 1 2^4 factorial design analysis of each factor and obtained FAME yield.

Table 2 Box-Behnken design for 3 factors with experimental and predicted FAME yields.

Table 3 Physicochemical properties of catalyst.

Table 4 Reaction rate constants for the ultrasonic assisted transesterification of waste cooking oil and methanol using CD-SO_3H catalyst at different temperatures.

Table 5 The properties of biodiesel in this work with ASTM D 6751 standard.

Figure captions

Fig. 1. (A) XRD patterns, (B) particle-size distribution, (C) SEM-EDS image, (D) TGA patterns, (E) FT-IR spectra, (F) XPS spectra and (G) NH_3-TPD profiles of catalyst.

Fig. 2. Normal probability plot of effect estimate for 2^4 factorial design.

Fig. 3. (A) Normal probability plot of residual and (B) distribution plot of residual versus predicted FAME yield for 2^4 factorial design.

Fig. 4. Plot of experimental versus predicted values of FAME yield. Distribution plot of residual versus predicted FAME yield for Box-Behnken design was inserted in this figure.

Fig. 5. The response surface plot of FAME yield: (A) based on catalyst loading and reaction time, (B) based on catalyst loading and reaction temperature, and (C) based on reaction time and reaction temperature.

Fig. 6. Water molecule obtained from esterification mechanism of free fatty acid with SO_3H-CD.

Fig. 7. Catalyst reusability in biodiesel production from waste cooking oil. Reaction condition: catalyst loading of 11.5 wt.%, reaction time of 8.8 min and reaction temperature of 117 °C.

Fig. 8. The first order reaction plot between time versus –ln(1-*X*).

Fig. 9. Arrhenius plot 1/*T* versus ln k'.

Table 1 2^4 factorial design analysis of each factor and obtained FAME yield.

Run	X_1 (wt.%)	X_2 (min)	X_3 (°C)	X_4 (mol/mol)	FAME yield (%)
1	5 (-1)	2 (-1)	50 (-1)	20:1 (-1)	20.9
2	15 (1)	2 (-1)	50 (-1)	20:1 (-1)	49.7
3	5 (-1)	14 (1)	50 (-1)	20:1 (-1)	54.1
4	15 (1)	14 (1)	50 (-1)	20:1 (-1)	59.9
5	5 (-1)	2 (-1)	150 (1)	20:1 (-1)	69.7
6	15 (1)	2 (-1)	150 (1)	20:1 (-1)	84.6
7	5 (-1)	14 (1)	150 (1)	20:1 (-1)	87.8
8	15 (1)	14 (1)	150 (1)	20:1 (-1)	85.5
9	5 (-1)	2 (-1)	50 (-1)	40:1 (1)	20.2
10	15 (1)	2 (-1)	50 (-1)	40:1 (1)	49.1
11	5 (-1)	14 (1)	50 (-1)	40:1 (1)	56.5
12	15 (1)	14 (1)	50 (-1)	40:1 (1)	60.4
13	5 (-1)	2 (-1)	150 (1)	40:1 (1)	69.6
14	15 (1)	2 (-1)	150 (1)	40:1 (1)	84.4
15	5 (-1)	14 (1)	150 (1)	40:1 (1)	86.9
16	15 (1)	14 (1)	150 (1)	40:1 (1)	84.4

The factors are coded as following: X_1 = catalyst loading (wt.%), X_2 = reaction time (min), X_3 = reaction temperature (°C) and X_4 = molar ratio of methanol to oil (mol/mol).

Table 2 Box-Behnken design for 3 factors with experimental and predicted FAME yields.

Run	X_1 (wt.%)	X_2 (min)	X_3 (°C)	FAME yield (%)	
				Experimental	Predicted
1	5 (-1)	2 (-1)	100 (0)	55.6	58.8
2	15 (1)	2 (-1)	100 (0)	72.1	71.5
3	5 (-1)	14 (1)	100 (0)	70.5	71.1
4	15 (1)	14 (1)	100 (0)	83.7	80.5
5	5 (-1)	8 (0)	50 (-1)	53.2	51.7
6	15 (1)	8 (0)	50 (-1)	65.9	68.1
7	5 (-1)	8 (0)	150 (1)	78.3	76.1
8	15 (1)	8 (0)	150 (1)	80.3	81.8
9	10 (0)	2 (-1)	50 (-1)	63.2	61.5
10	10 (0)	14 (1)	50 (-1)	75.4	76.4
11	10 (0)	2 (-1)	150 (1)	85.7	84.8
12	10 (0)	14 (1)	150 (1)	89.5	91.2
13	10 (0)	8 (0)	100 (0)	85.3	85.6
14	10 (0)	8 (0)	100 (0)	85.5	85.6
15	10 (0)	8 (0)	100 (0)	85.9	85.6

The factors are coded as following: X_1 = catalyst loading (wt.%), X_2 = reaction time (min) and X_3 = reaction temperature (°C).

Table 3 Physicochemical properties of catalyst.

CD-SO_3H	BET Surface area (m^2/g)	Pore size (nm)	Acidity (mmol/g)	S (wt.%)	C (wt.%)	O (wt.%)
Fresh catalyst	8.2	22.1	1.87	5.98	85.80	8.22
Spent catalyst[a]	8.4	18.5	1.85	5.91	86.23	7.86
Spent catalyst[b]	7.8	17.4	1.51	4.13	88.9	6.97

[a] After regeneration (4th reuse).

[b] Without regeneration (4th reuse)

Table 4 Reaction rate constants for the ultrasonic assisted transesterification of waste cooking oil and methanol using CD-SO_3H catalyst at different temperatures.

Temperature (°C)	Reaction rate constant (min^{-1})	R^2
60	0.0472	0.9918
80	0.0581	0.9905
100	0.0751	0.9911
120	0.0884	0.9934

Table 5 The properties of biodiesel in this work with ASTM D 6751 standard.

Properties	Unit	Value	
		Biodiesel (ASTM 6751)	Biodiesel (This work)
Density@15 °C	g/cm^3	0.86-0.89	0.8766
Viscosity@15 °C	mm^2/s	1.9-6.0	4.15
Oxidative stability@110 °C	h	≥3	2.6
Pour point	°C	-10 to 12	2
Flash point	°C	≥130	194
Heating value	cal/g	9940	9912
Cetane number		≥47	50
Acid value	(KOH mg/kg)	≤0.5	0.45
Sulfur content	(%, w/w)	≤0.05	0.003
Water content	(mg/kg)	≤0.05	0.0045

1 **Figure 1**

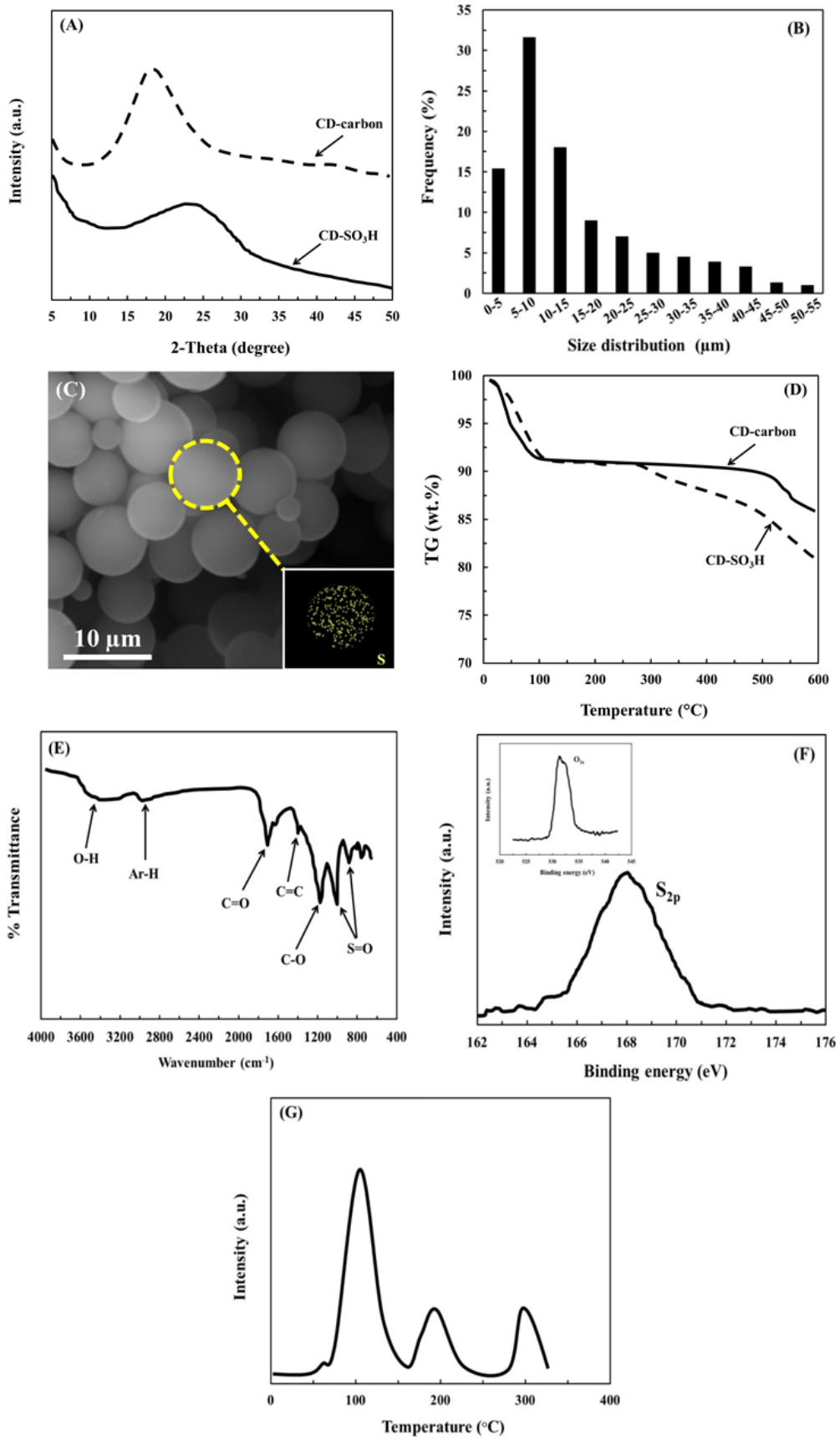

2

Figure 2

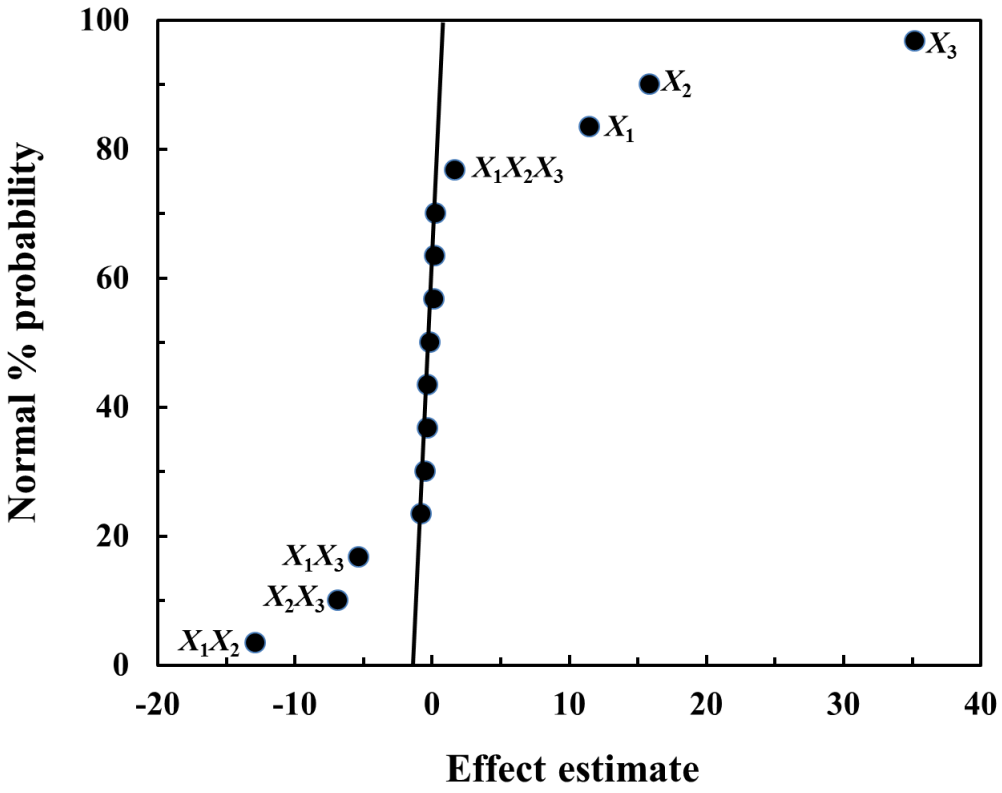

1 **Figure 3**

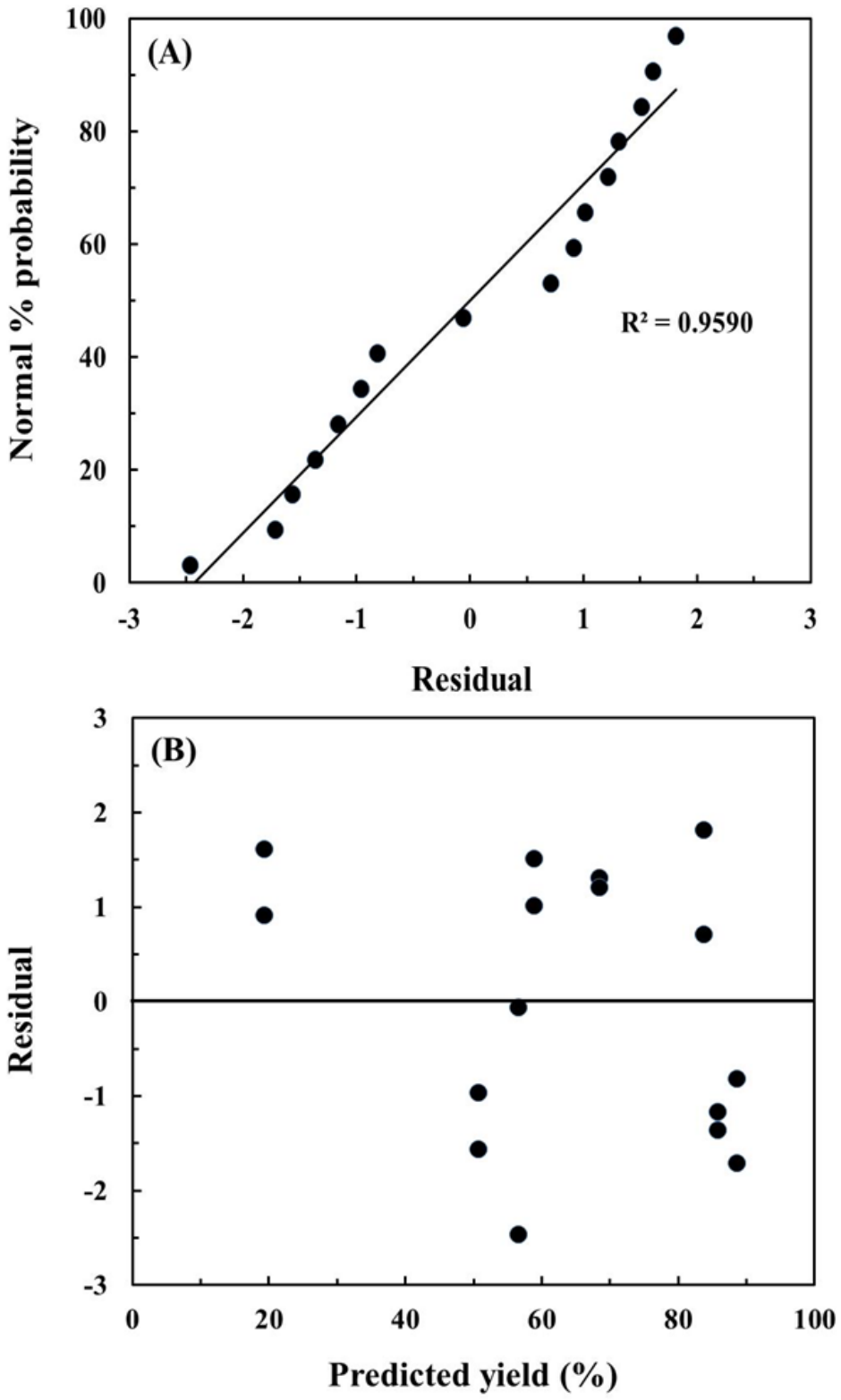

2

3

Figure 4

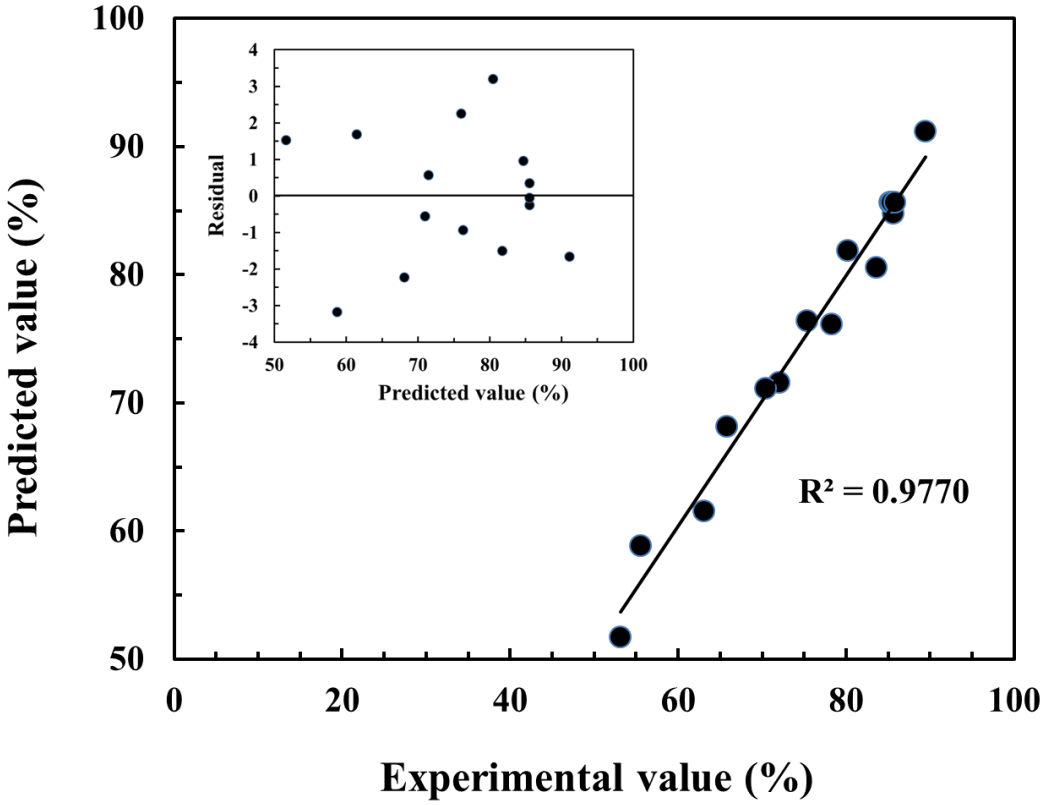

Figure 5

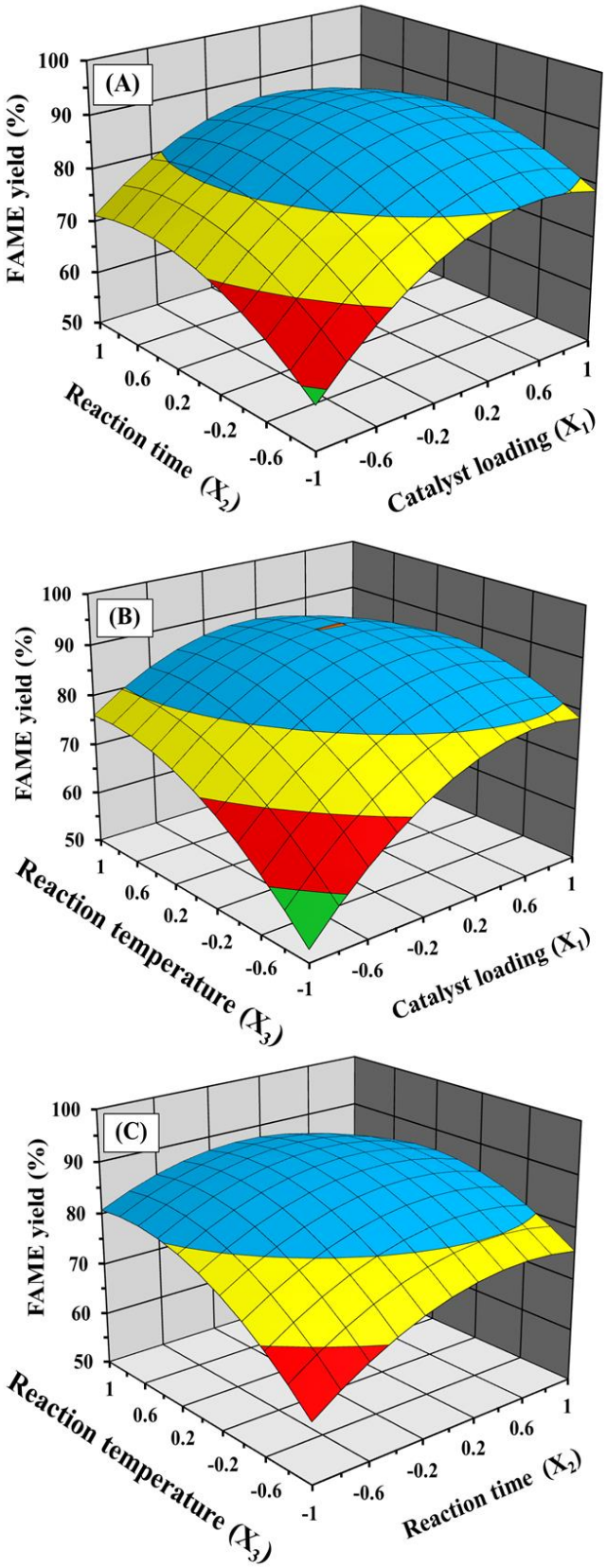

Figure 6

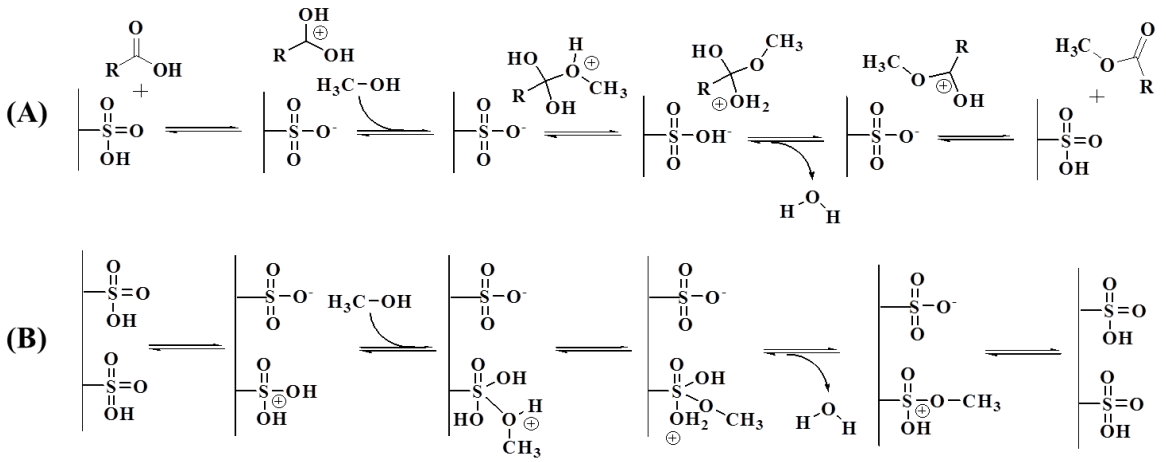

Figure 7

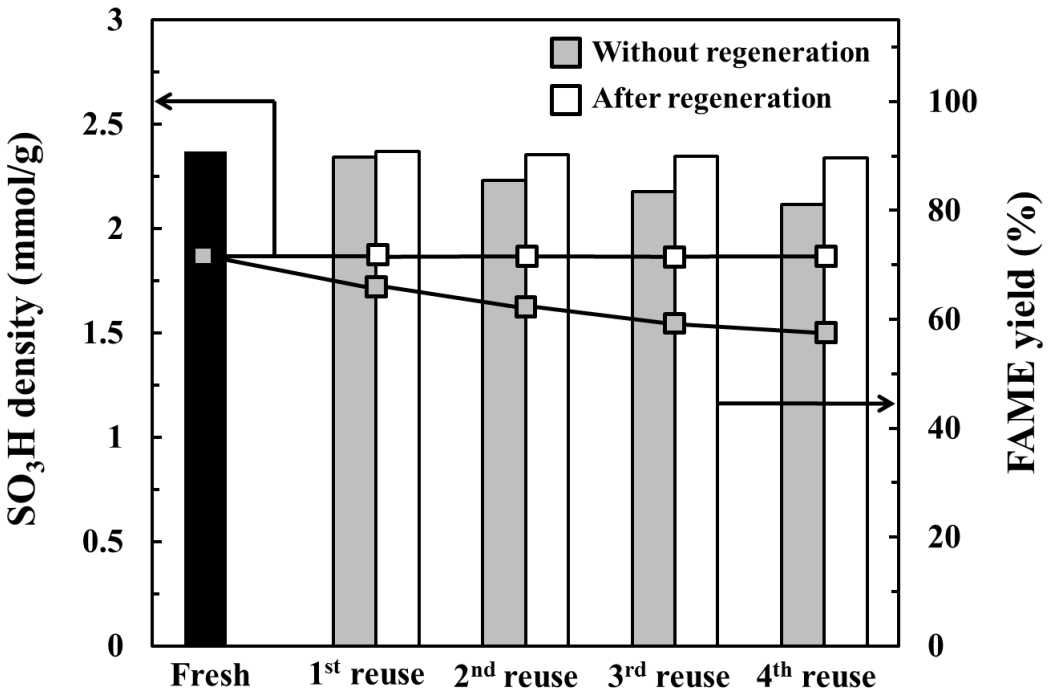

Figure 8

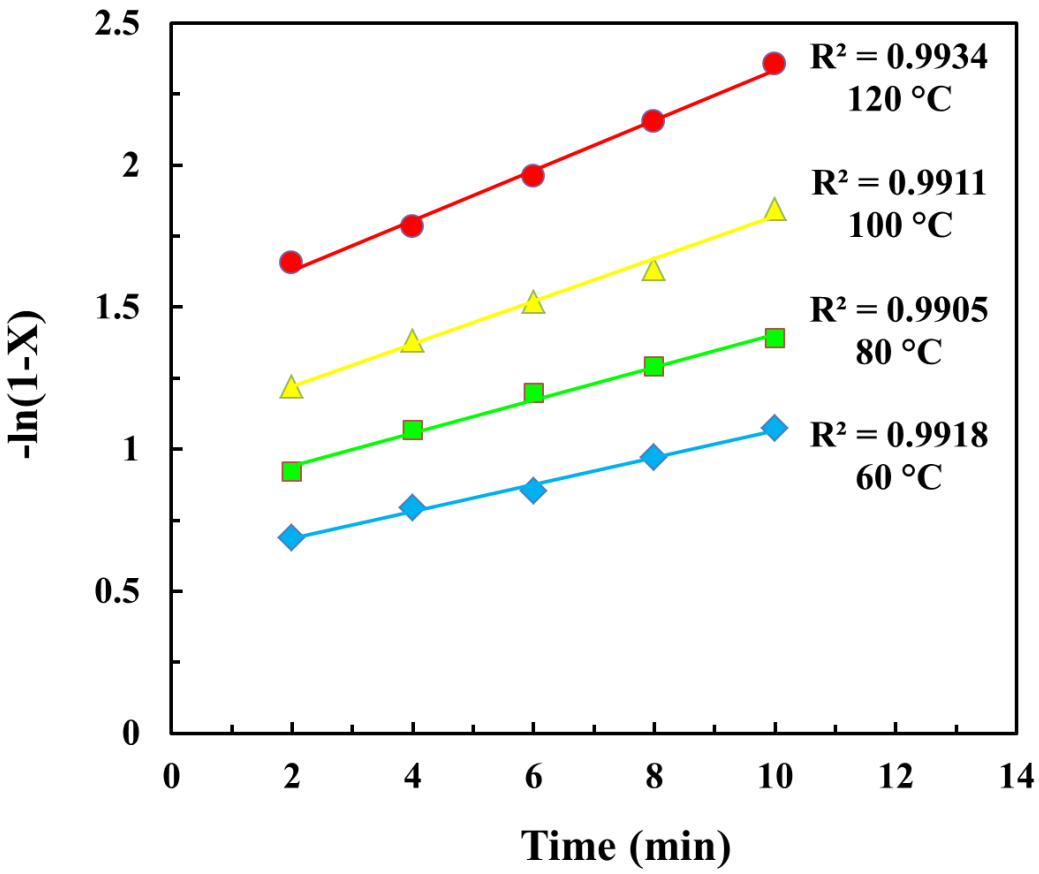

Figure 9

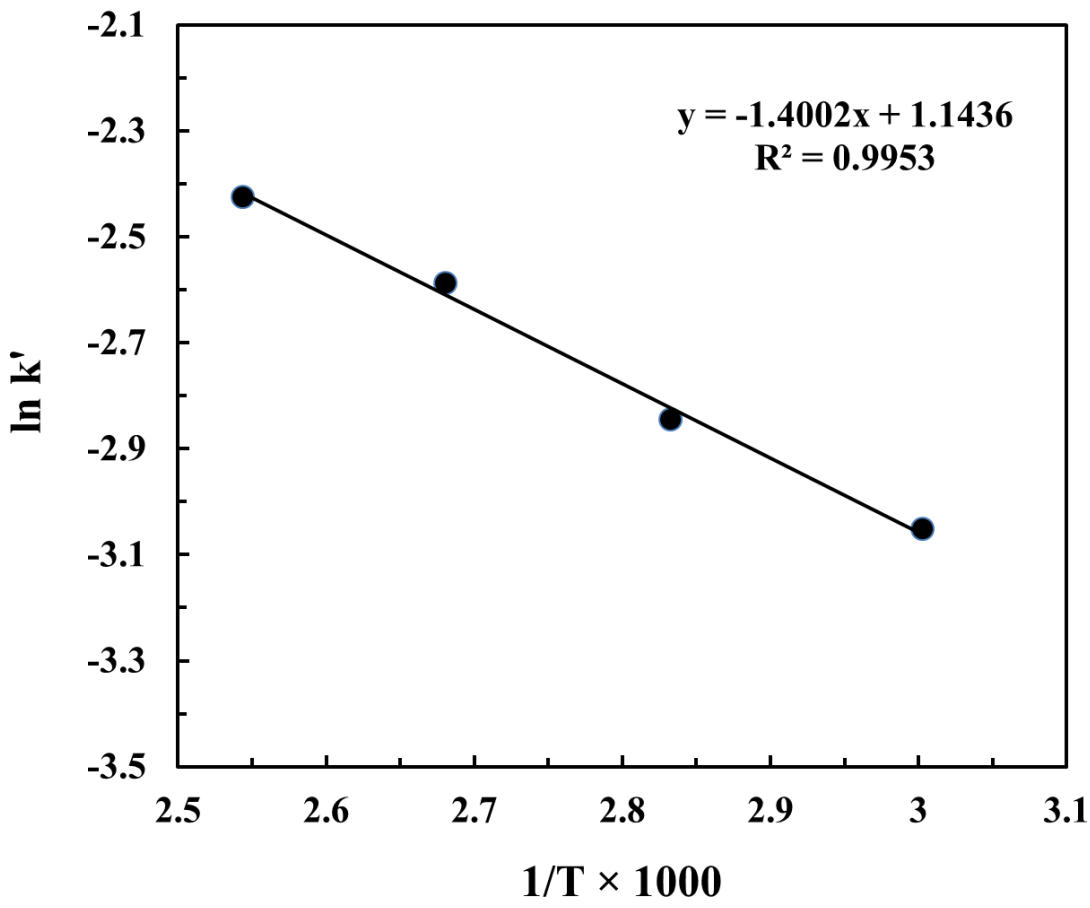

Table of contents entry

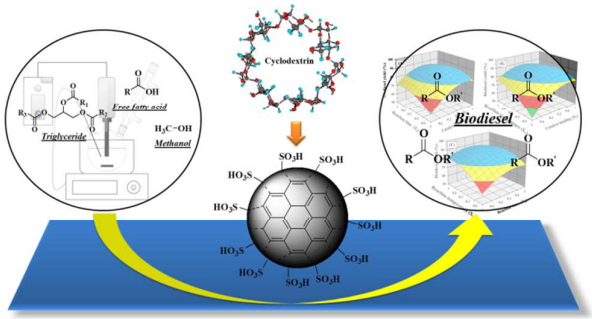

A novel sulfonated carbon derived from cyclodextrin showed high catalytic activity for the ultrasonic assisted transesterification of waste cooking oil.